Ligand-Dependent Interaction of PPARδ With T-Cell Protein Tyrosine Phosphatase 45 Enhances Insulin Signaling

Taesik Yoo,[1] Sun Ah Ham,[1] Won Jin Lee,[1] Seon In Hwang,[2] Jin-A Park,[3] Jung Seok Hwang,[1] Jinwoo Hur,[1] Ho-Chul Shin,[3] Sung Gu Han,[1] Chi-Ho Lee,[1] Dong Wook Han,[2] Kyung Shin Paek,[4] and Han Geuk Seo[1]

Diabetes 2018;67:360–371 | https://doi.org/10.2337/db17-0499

METABOLISM

Peroxisome proliferator–activated receptor (PPAR) δ plays a pivotal role in metabolic homeostasis through its effect on insulin signaling. Although diverse genomic actions of PPARδ are postulated, the specific molecular mechanisms whereby PPARδ controls insulin signaling have not been fully elucidated. We demonstrate here that short-term activation of PPARδ results in the formation of a stable complex with nuclear T-cell protein tyrosine phosphatase 45 (TCPTP45) isoform. This interaction of PPARδ with TCPTP45 blocked translocation of TCPTP45 into the cytoplasm, thereby preventing its interaction with the insulin receptor, which inhibits insulin signaling. Interaction of PPARδ with TCPTP45 blunted interleukin 6–induced insulin resistance, leading to retention of TCPTP45 in the nucleus, thereby facilitating deactivation of the signal transducer and activator of transcription 3 (STAT3)–suppressor of cytokine signaling 3 (SOCS3) signal. Finally, GW501516-activated PPARδ improved insulin signaling and glucose intolerance in mice fed a high-fat diet through its interaction with TCPTP45. This novel interaction of PPARδ constitutes the most upstream component identified of the mechanism downregulating insulin signaling.

Insulin initiates its cellular actions by binding to its cell surface transmembrane receptor, which is a tyrosine kinase (1). Upon binding of insulin to the extracellular α-subunit, the intrinsic protein tyrosine kinase (PTK) activity of the intracellular β-subunit is activated, leading to its autophosphorylation and subsequent phosphorylation of insulin receptor (IR) substrate (IRS) proteins and other adaptor molecules (2). This tyrosine phosphorylation provides docking sites for the recruitment of several src homology 2 domain–containing proteins, such as the p85 regulatory subunit of phosphatidylinositol 3-kinase (PI3K), which mediate the biological activities of insulin in its target organs (2,3). Under the pathological conditions associated with obesity and type 2 diabetes, impaired responses to insulin are coupled with resistance to its actions in target organs, including liver, muscle, and adipose tissue (3).

Evidence is emerging that protein tyrosine phosphatases (PTPs) play a pivotal role in IR signaling by dephosphorylating the IR within minutes of its activation to terminate IR-mediated insulin signaling (4,5). T-cell protein tyrosine phosphatase (TCPTP) and PTP1B are both implicated as negative regulators of IR (4,6), but they have distinct biological activities by virtue of their substrate specificity and different subcellular locations (4). TCPTP, which was originally identified in human T cells (7), has two alternative splice variants: a 48-kDa form (TCPTP48), which contains a hydrophobic carboxy-terminus and is localized to the endoplasmic reticulum (ER), similar to PTP1B, and a shorter 45-kDa form (TCPTP45), which lacks the hydrophobic C-terminus and is targeted to the nucleus (8).

TCPTP45 is localized to the nucleus in resting cells but is translocated to the cytoplasm and plasma membrane in response to external stimuli, such as insulin, where it can access its substrates (9). Accordingly, TCPTP45 can dephosphorylate the IR in the cytoplasm and at the plasma membrane, whereas ER-targeted TCPTP48 dephosphorylates the IR after it has been endocytosed, similar to the action of

[1]Sanghuh College of Life Sciences, Konkuk University, Seoul, Korea
[2]Department of Stem Cell Biology, Konkuk University, Seoul, Korea
[3]Department of Veterinary Pharmacology and Toxicology, Konkuk University, Seoul, Korea
[4]Department of Nursing, Semyung University, Jechon, Korea
Corresponding author: Han Geuk Seo, hgseo@konkuk.ac.kr.

Received 26 April 2017 and accepted 27 November 2017.

This article contains Supplementary Data online at http://diabetes.diabetesjournals.org/lookup/suppl/doi:10.2337/db17-0499/-/DC1.

PTP1B (5,9). In addition to using receptor PTKs such as IR as substrates, TCPTP also uses nonreceptor PTKs as substrates, including signal transducer and activator of transcription 3 (STAT3) (10,11). Indeed, recent studies demonstrated that STAT3, a target of TCPTP45, is implicated in the insulin resistance induced by interleukin 6 (IL-6) through upregulation of suppressor of cytokine signaling 3 (SOCS3), which contributes to the negative regulation of insulin signaling by interacting with the IR and IRS (12).

The biological activity of peroxisome proliferator–activated receptor (PPAR) δ, a nuclear receptor, has been credited to transcriptional programs that regulate the expression of target genes (the so-called genomic action) (13,14). However, there have been recent reports that could not explain the biological functions of PPARδ by a genomic action alone (15,16). Here, we report that short-term activation of PPARδ by high-affinity ligand results in the formation of a stable complex with TCPTP45, thereby blocking the insulin-responsive translocation of nuclear TCPTP45 into the cytoplasm and preventing access of TCPTP45 to IR and its inhibitory effect on insulin signaling. In addition, this protein-protein interaction blunts IL-6–induced insulin resistance by accelerating TCPTP45-mediated deactivation of the STAT3-SOCS3 signal in a process mediated by sequestration of TCPTP45 within the nuclear compartment. These observations demonstrate the role of a novel TCPTP45-mediated pathway in the insulin-sensitizing action of PPARδ.

RESEARCH DESIGN AND METHODS

Coimmunoprecipitation and Immunoblot Analysis

Cell and tissue lysates were prepared and then precleared with protein G Sepharose. Precleared lysates were mixed with the specified antibodies and then precipitated with protein G Sepharose. The immunoprecipitates and total lysates (input) were washed with PBS and analyzed by immunoblot.

Animal Study

Male ICR mice (4 weeks old, 15–20 g) were purchased from Orient Bio (Seongnam, Korea) and maintained in pathogen-free environmental conditions on a 12-h light-dark cycle at 22 ± 2°C. All procedures were approved by the Konkuk University Institutional Animal Care and Use Committee (approval number: KU16144). After 1 week of acclimation, the mice were divided into two groups and were fed a normal diet (ND) (Altromin Spezialfutter GmbH & Co., Lage, North Rhine-Westphalia, Germany) or a high-fat diet (HFD) (Research Diets, New Brunswick, NJ) for 10 weeks, during which water and diet were available ad libitum.

Glucose and Insulin Tolerance Tests

For intraperitoneal glucose tolerance testing, mice were fasted for 16 h, and then glucose (2 g/kg body mass) was administered intraperitoneally. Blood was taken from the tail vein at 0, 30, 60, 90, and 120 min after the glucose injection, and the circulating glucose levels were determined using a OneTouch automatic glucose monitor (LifeScan, Milpitas, CA). For intraperitoneal insulin tolerance testing (IPITT), insulin (0.5 units/kg of body mass) in sterile saline was injected intraperitoneally, and the circulating glucose levels were determined as described above.

Statistical Analysis

Data are expressed as mean ± SE. Statistical significance was determined by one-way ANOVA, followed by the Tukey-Kramer or Student *t* test, as appropriate.

RESULTS

PPARδ Directly Interacts With TCPTP45

In a yeast-hybrid assay that used PPARδ as bait, we identified a cDNA fragment encoding a full-length amino acid sequence of TCPTP45 in a universal human cDNA library. The interaction of PPARδ with TCPTP45 was confirmed by coimmunoprecipitation assays performed in primary hepatocytes, hepatoblastoma-derived HepG2 cells, differentiated C2C12 myotubes, and 3T3-L1 adipocytes. When cells were treated with GW501516, a specific PPARδ agonist, immunoprecipitation of PPARδ from whole-cell lysates resulted in the coimmunoprecipitation of TCPTP45. However, PTP1B, another tyrosine-specific phosphatase that targets the IR β-subunit (IRβ), was not coimmunoprecipitated with PPARδ (Fig. 1*A–D*). This GW501516-dependent interaction was almost completely abolished in HepG2 cells stably expressing PPARδ small hairpin (sh)RNA, indicating that ligand-dependent activation of PPARδ is a prerequisite for its interaction with TCPTP45 (Fig. 1*E* and Supplementary Fig. 1*A*). This interaction of PPARδ with TCPTP45 was also confirmed using reciprocal antibodies for immunoprecipitation and immunoblotting (Fig. 1*F*). No proteins were immunoprecipitated using control IgG. Similar results were obtained in HEK293T cells cotransfected with Flag-tagged PPARδ and hemagglutinin (HA)-tagged TCPTP45, in which the GW501516-dependent interaction of PPARδ and TCPTP45 was present at 30 min and reached a maximum at 45 min (Fig. 1*G* and Supplementary Fig. 1*B*). In addition, when HEK293T cells were transfected with individual plasmids expressing PPARα, δ, or γ, together with TCPTP45, in the presence or absence of specific ligands for each PPAR isoform, PPARδ but not PPARα and γ demonstrated a strong interaction with TCPTP45 in a coimmunoprecipitation assay, indicating that only the PPARδ isoform can interact with TCPTP45 (Supplementary Fig. 1*C*).

The Bipartite Nuclear Localization Sequence of TCPTP45 Is Responsible for Its Interaction With PPARδ

A direct interaction between PPARδ and TCPTP45 was further confirmed in glutathione *S*-transferase (GST) pull-down assays, in which most of the PPARδ was pulled down with GST-fused TCPTP45 in the presence of GW501516 (Fig. 2*A*). Thus, we generated a panel of TCPTP45 deletion mutants to identify the regions of TCPTP45 that are responsible for its interaction with PPARδ (Fig. 2*B*). Whereas full-length TCPTP45 (FL) displayed a strong interaction with PPARδ, the deletion mutants TCPTP45 (D1) and TCPTP45 (D2) showed no significant interaction, indicating

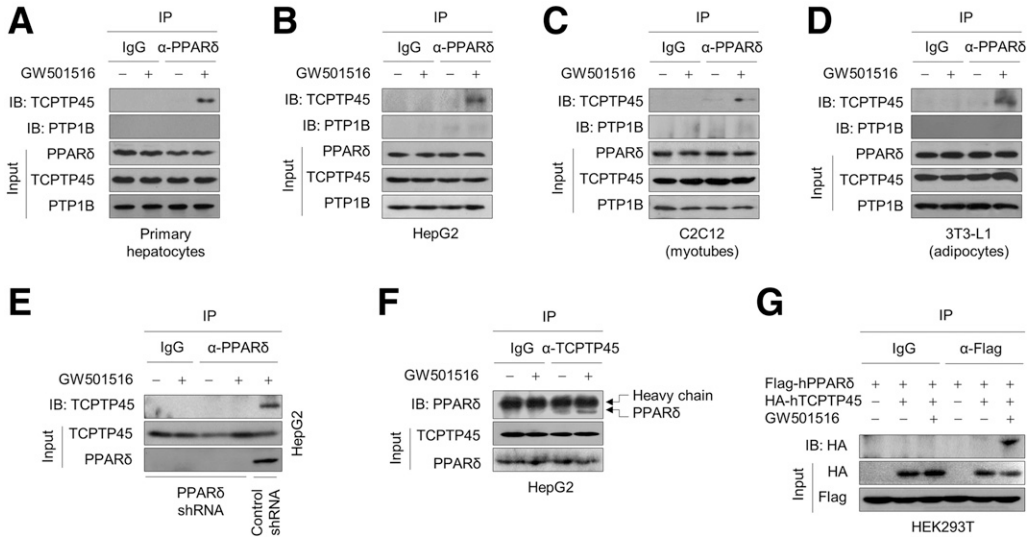

Figure 1—PPARδ directly interacts with TCPTP45. Primary hepatocytes (*A*), HepG2 cells (*B*), C2C12 myotubes (*C*), or 3T3-L1 adipocytes (*D*) were treated with 100 nmol/L GW501516 or DMSO for 45 min, and then whole-cell lysates were prepared and immunoprecipitated (IP) with IgG or anti-PPARδ antibody. The immunoprecipitates and total lysates (input) were subjected to immunoblot (IB) analysis with specific antibodies to detect the indicated proteins. Two percent of each whole-cell lysate was used as the input. *E*: HepG2 cells stably expressing control shRNA or shRNA targeting PPARδ were treated with 100 nmol/L GW501516 or DMSO for 45 min. Whole-cell lysates were immunoprecipitated with IgG or anti-PPARδ antibody and analyzed by immunoblotting. *F*: HepG2 cells treated with 100 nmol/L GW501516 or DMSO for 45 min were lysed and immunoprecipitated with IgG or anti-TCPTP45 antibody. The immunoprecipitates and total lysates (input) were subjected to immunoblot analysis. *G*: HEK293T cells cotransfected with Flag-human PPARδ (Flag-hPPARδ) and/or HA-human TCPTP45 (HA-hTCPTP45) for 48 h were treated with 100 nmol/L GW501516 or DMSO for 45 min, and then whole-cell lysates were prepared and immunoprecipitated with IgG or anti-Flag antibody.

that the COOH-terminal region of TCPTP45 is essential for this interaction (Fig. 2*C*). Because the COOH-terminal region of TCPTP45 has a bipartite nuclear localization sequence (NLS), we constructed three NLS mutants to identify the critical amino acid residue(s) responsible for the association of TCPTP45 with PPARδ. Site-directed mutants were constructed by introducing amino acid substitutions in the N-terminal part of NLS residues 350, 351, and 352 of TCPTP45 ($TCPTP45^{350\text{-}A3}$), and further substitutions in the COOH-terminal part of NLS residues 378, 379, and 380 ($TCPTP45^{378\text{-}A3}$), and in both the N- and COOH-terminal parts of NLS residues 350, 351, 352, 378, 379, and 380 ($TCPTP45^{350/378\text{-}A3}$), replacing arginine or lysine residues with alanine (Fig. 2*D*).

When these mutant proteins were individually incubated with lysates prepared from HEK293T cells that had been transfected with PPARδ, $TCPTP45^{350\text{-}A3}$ displayed a weaker ability than $TCPTP45^{378\text{-}A3}$ to interact with PPARδ. Furthermore, the interaction between PPARδ and TCPTP45 was nearly eliminated when PPARδ was incubated with $TCPTP45^{350/378\text{-}A3}$, indicating that the bipartite NLS of TCPTP45 is indispensable for the interaction with PPARδ (Fig. 2*E*). Consistent with this, the localization of TCPTP45 was limited to the cytoplasm of HepG2 cells transfected with HA-tagged $TCPTP45^{350/378\text{-}A3}$ (Fig. 2*F*).

Because TCPTP48 also has a bipartite NLS region, we examined the association between PPARδ and TCPTP48 in HepG2 by coimmunoprecipitation. As expected, PPARδ interacted with TCPTP48, suggesting that such protein-protein interactions via the bipartite NLS region may occur nonspecifically under any conditions in which these molecules come close together by cellular destruction (Supplementary Fig. 2*A*). However, when the nuclear or cytoplasmic fractions of HepG2 cells stimulated with GW501516 were analyzed to confirm the specificity of TCPTP, an interaction between PPARδ and TCPTP was observed in both fractions (Supplementary Fig. 2*B* and *C*). These results indicate that although TCPTP45 and TCPTP48 can both interact with PPARδ via their bipartite NLS, their subcellular location is a unique determinant for a specific interaction with PPARδ.

To further evaluate the specificity of the bipartite NLS of TCPTP45 in the interaction with PPARδ, the bipartite NLS of TCPTP45 was replaced with SV40 large T antigen NLS (17). When the cells were transfected with $TCPTP45^{350/378\text{-}SV40}$, although most of $TCPTP45^{350/378\text{-}SV40}$ was observed in the nuclear fraction, the interaction between PPARδ and $TCPTP45^{350/378\text{-}SV40}$ was not detected in the presence of GW501516 (Supplementary Fig. 2*D*–*F*).

GW501516-Activated PPARδ Inhibits the Insulin-Triggered Translocation of TCPTP45 From Nucleus to Cytoplasm

Because PPARδ interacted with both TCPTP45 and TCPTP48 in lysates prepared from HepG2 cells, we examined the cellular colocalization of PPARδ and TCPTPs to confirm the exact nature of the interaction with PPARδ. By confocal fluorescence microscopy using fluorescent fusion protein versions of PPARδ and $TCPTP45^{D182A}$ or $TCPTP48^{D182A}$, which are substrate-trapping mutants that can form complexes with

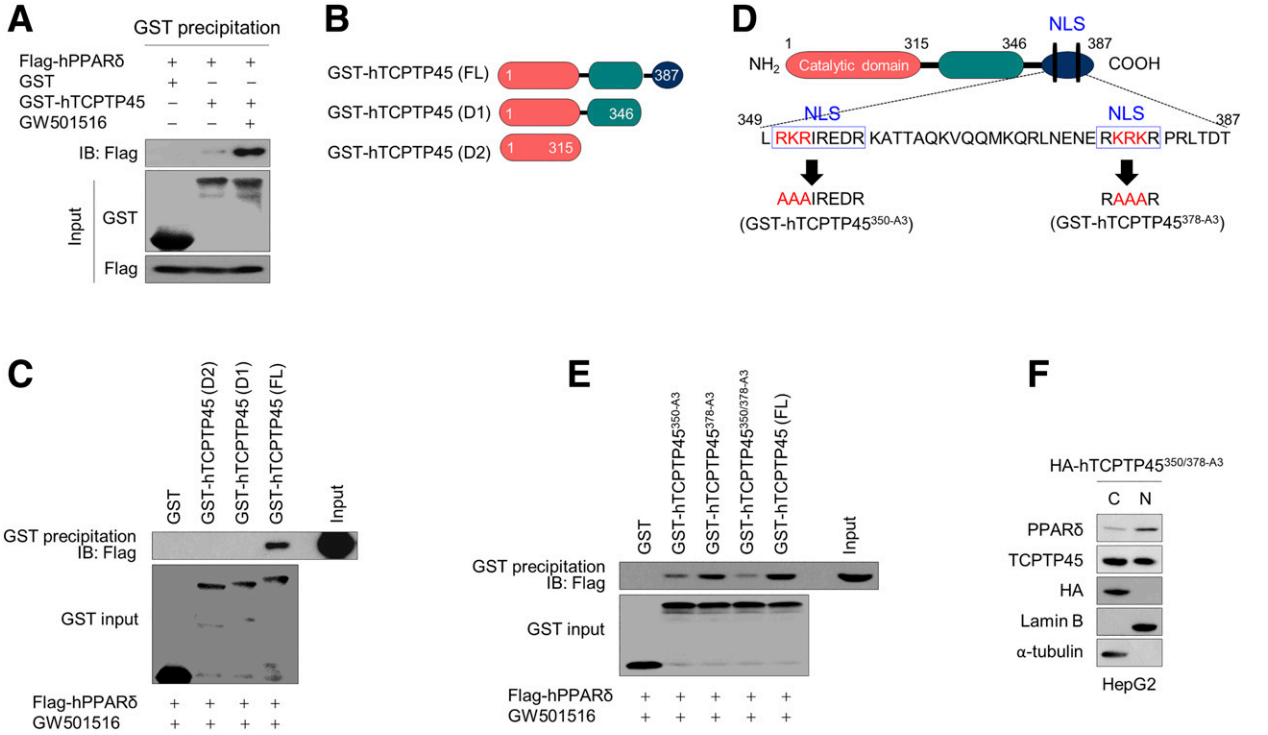

Figure 2—PPARδ targets the bipartite nuclear localization signal of TCPTP45. Whole-cell lysates prepared from HEK293T cells transfected with Flag-human PPARδ (Flag-hPPARδ) for 48 h were incubated with recombinant GST or GST-human TCPTP45 (GST-hTCPTP45) fusion protein (*A*), GST or GST-fused deletion mutants (*C*), or GST or GST-fused site-directed mutants (*E*) immobilized to glutathione-Sepharose 4B beads for 20 h in the presence of 100 nmol/L GW501516 or DMSO. Bead-bound proteins were analyzed by immunoblotting. Two percent of each whole-cell lysate was used as the input. *B*: Schematic illustrations of GST-hTCPTP45 fusion protein constructs. *D*: Schematic illustration of the COOH-terminal bipartite NLS region of TCPTP45. *F*: HepG2 cells were transfected with pcDNA-HA-hTCPTP45$^{350/378\text{-}A3}$ for 48 h and then separated into nuclear (N) and cytoplasmic (C) fractions. Each fraction was then subjected to immunoblot (IB) analysis.

tyrosine-phosphorylated substrates (18), we observed that green fluorescent protein (GFP)–tagged PPARδ was colocalized with *Discosoma* spp. red fluorescent protein (DsRed)–tagged TCPTP45 in the nucleus of CHO cells stably expressing the IR (CHO-IR). Upon stimulation with insulin, most of the DsRed-TCPTP45 was rapidly translocated into the cytoplasm, but this insulin-stimulated translocation was almost completely abolished in cells treated with GW501516 (Supplementary Fig. 3*A*). By contrast, neither colocalization of GFP-PPARδ and DsRed-TCPTP48 nor translocation between intracellular compartments was observed, stressing the importance of subcellular localization in the interaction between PPARδ and TCPTP45 (Supplementary Fig. 3*B*).

To investigate whether GW501516-activated PPARδ affects the insulin-stimulated interaction of TCPTP45 with IRβ, coimmunoprecipitation assays were performed using Flag-PPARδ and HA-TCPTP45^{D182A} in CHO-IR and HepG2 cells. Upon stimulation with insulin, IRβ was coimmunoprecipitated with TCPTP45^{D182A} in both cells, whereas an interaction between PPARδ and TCPTP45^{D182A} was not observed in the absence of GW501516. By contrast, insulin-stimulated complex formation between IRβ and TCPTP45^{D182A} was reduced in cells treated with GW501516 because of increased interaction between PPARδ and TCPTP45^{D182A}. Furthermore, GSK0660-mediated antagonism of GW501516 caused the dissociation of PPARδ and TCPTP45^{D182A}, with a concomitant increase in the formation of IRβ and TCPTP45^{D182A} complexes (Fig. 3*A* and *B*). Similar results were obtained from HepG2 cells stably expressing PPARδ or control shRNA (Fig. 3*C*). As expected, insulin-stimulated translocation of TCPTP45^{D182A} from the nucleus to the cytoplasm was almost completely abolished in the presence of GW501516 with a concomitant reduction in the interaction of TCPTP45^{D182A} and phosphorylated IRβ, and this GW501516-mediated inhibition of TCPTP45^{D182A} translocation and interaction with IRβ was prevented by GSK0660 (Fig. 3*D*).

The GW501516-Stimulated Interaction of PPARδ With TCPTP45 Potentiates the Insulin Signal

GW501516 induced an interaction between PPARδ and TCPTP45; thus, particular attention was paid to the effect on insulin signaling because TCPTP45 can antagonize insulin signaling by dephosphorylating IRβ (5). When HepG2 cells were treated with insulin, IRβ was rapidly phosphorylated, and this effect was further potentiated in the presence of GW501516 (Fig. 4*A*). This GW501516-mediated potentiation of IRβ phosphorylation was almost completely abolished in HepG2 cells transfected with TCPTP45$^{350/378\text{-}A3}$, a site-directed mutant lacking the molecular regions that interact with PPARδ (Fig. 4*B*). Consistent with these results,

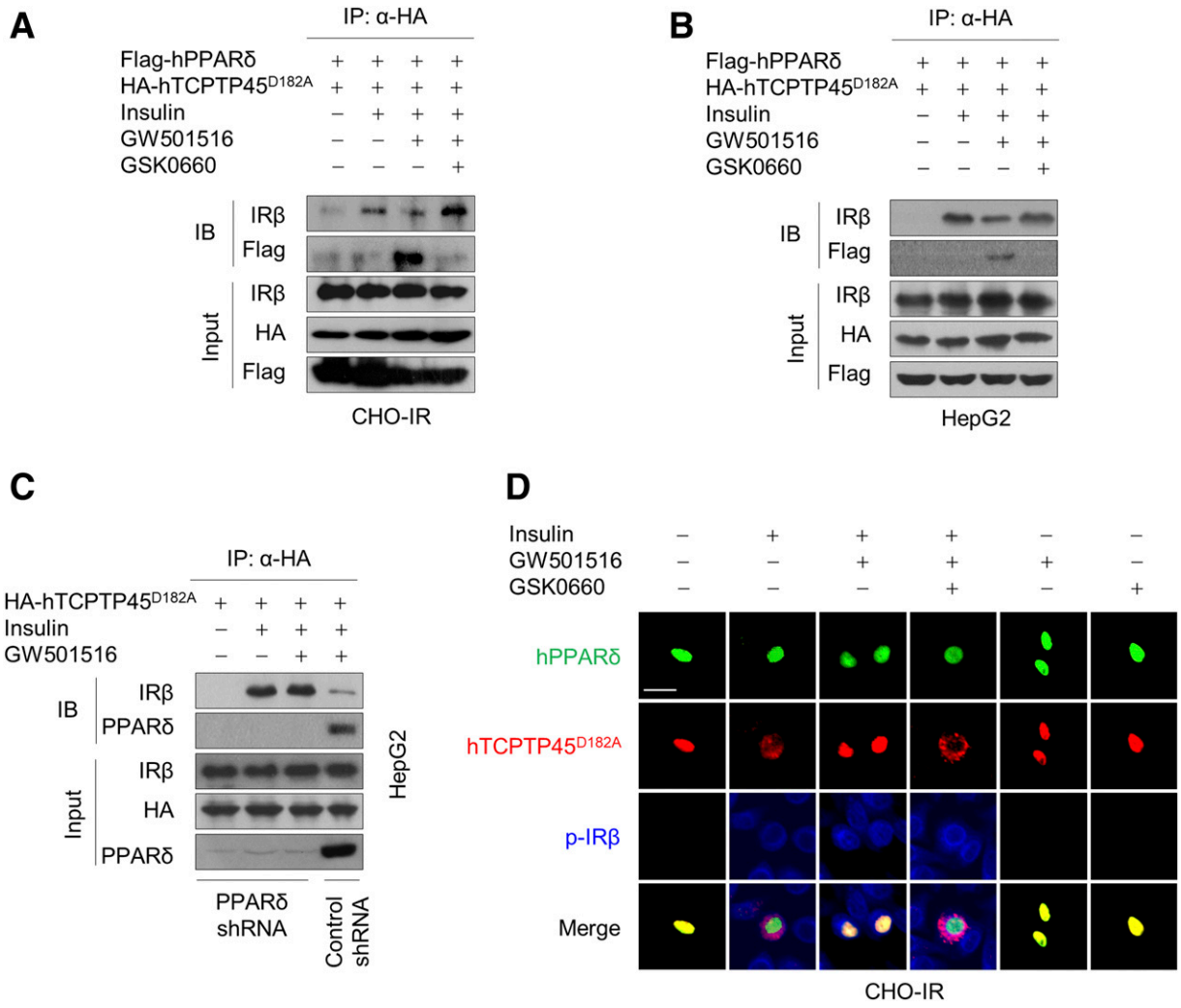

Figure 3—GW501516-activated PPARδ inhibits insulin-stimulated translocation of TCPTP45 from the nucleus to the cytoplasm. CHO-IR (*A*) or HepG2 cells (*B*) cotransfected with Flag-PPARδ and HA-human (h) TCPTP45^{D182A} for 48 h were treated with 1 μmol/L GSK0660 or DMSO for 30 min and then treated with 100 nmol/L GW501516. After incubation for a further 30 min, the cells were exposed to 100 nmol/L insulin for a final 30 min. *C*: HepG2 cells stably expressing PPARδ or control shRNA were transfected with HA-hTCPTP45^{D182A} for 48 h and then treated with 100 nmol/L GW501516 for 30 min. After exposure to 100 nmol/L insulin for a final 30 min, whole-cell lysates were immunoprecipitated and analyzed by immunoblot (IB) analysis. Two percent of each whole-cell lysate was used as the input. IP, immunoprecipitation. *D*: CHO-IR cells cotransfected with GFP-PPARδ and DsRed-hTCPTP45^{D182A} for 48 h were incubated with 1 μmol/L GSK0660 or DMSO for 30 min and then treated with 100 nmol/L GW501516 and incubated for 30 min. After exposure to 100 nmol/L insulin for a final 30 min, the colocalization of TCPTP45 with PPARδ or phosphorylated (p) IRβ is indicated by the presence of yellow or pink in the merged image, respectively. For phosphorylated IRβ, the fixed cells were sequentially reacted with primary anti-phosphorylated IRβ antibody and Alexa Fluor 680–conjugated secondary antibody, and then the fluorescent signals were visualized. Scale bar = 20 μm.

GW501516-mediated potentiation of IRβ phosphorylation was also manifested in cells that transiently expressed TCPTP45 but not TCPTP48 (Fig. 4*C*). Furthermore, small interfering (si)RNA-mediated silencing of TCPTP, but not PTP1B, prevented the effect of GW501516 to potentiate IRβ phosphorylation (Fig. 4*D* and Supplementary Fig. 4*A*). Similar results are shown in primary hepatocytes (Fig. 4*E*).

GW501516-Activated PPARδ Extends the Duration of Insulin-Stimulated IRβ Phosphorylation

When HepG2 cells were exposed to insulin, IRβ phosphorylation peaked after 2–5 min and then rapidly returned to basal levels. However, pretreatment with GW501516 for 30 min sustained IRβ phosphorylation until 60 min after the initial insulin exposure (Fig. 4*F* and *H*). This effect of GW501516 on the duration of IRβ phosphorylation was further potentiated in cells ectopically expressing PPARδ (Fig. 4*G* and *H*, and Supplementary Fig. 4*B* and *C*). This effect of GW501516 remained significant for as long as 6 h in cells expressing PPARδ (Supplementary Fig. 4*D*). This effect of GW501516 on IRβ phosphorylation was prevented by shRNA-mediated silencing of PPARδ (Fig. 4*I*–*K*) but was rescued by ectopic overexpression of PPARδ in transfectants stably expressing PPARδ shRNA (Fig. 4*L*–*N*). By contrast, treatment with WY14643 or rosiglitazone, specific ligands

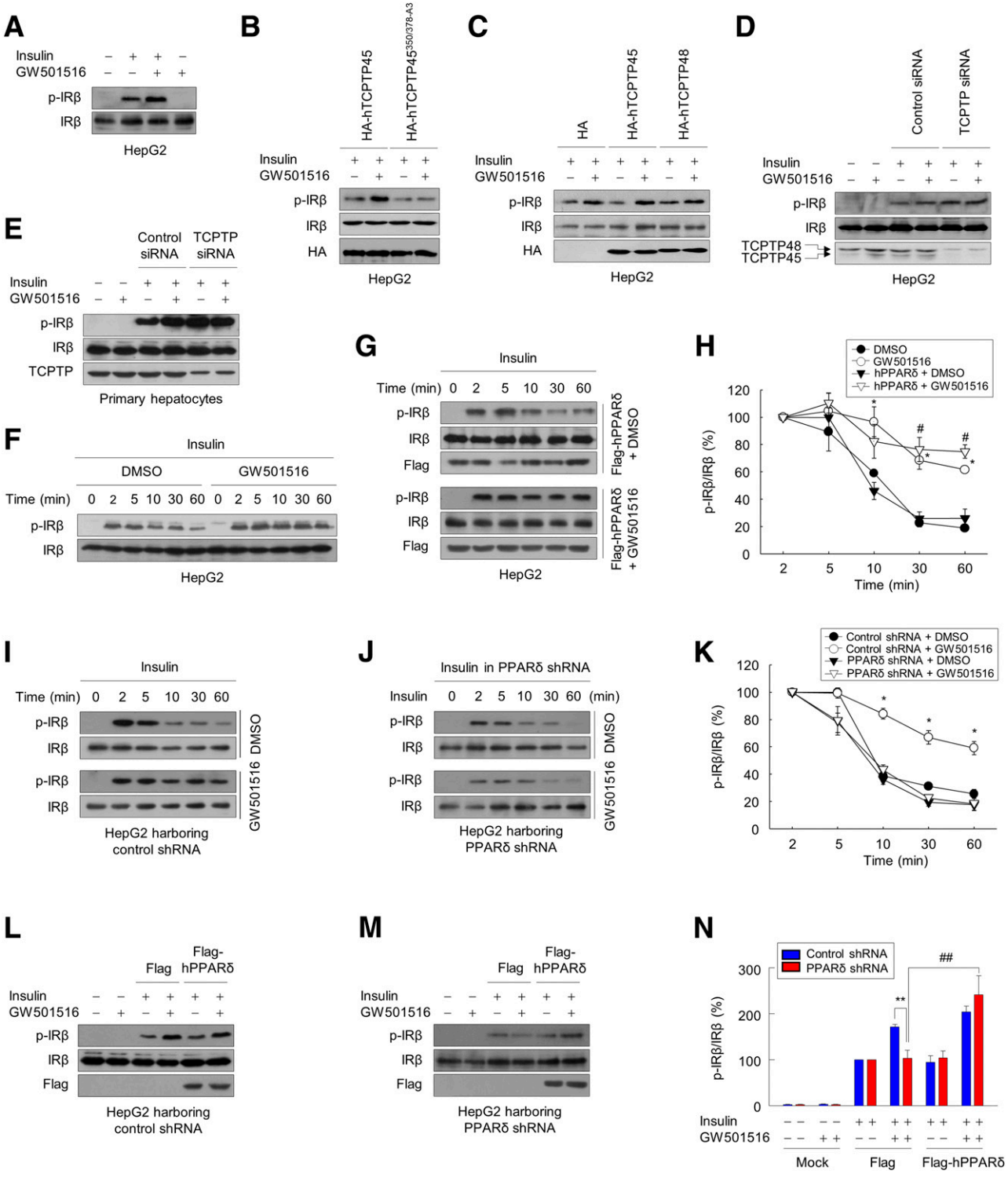

Figure 4—GW501516-activated PPARδ extends the duration of insulin-stimulated IRβ phosphorylation (p-IRβ). *A*: HepG2 cells were treated with 100 nmol/L GW501516 or DMSO for 30 min and then treated with or without 100 nmol/L insulin for a further 30 min. Whole-cell lysates were prepared and subjected to immunoblot analysis. HepG2 cells cotransfected with HA-tagged plasmids expressing human TCPTP45 (hTCPTP45) or hTCPTP45$^{350/378\text{-A3}}$ (*B*) or hTCPTP45 or hTCPTP48 (*C*) for 48 h were treated with 100 nmol/L GW501516 or DMSO for 30 min and then exposed to insulin for a further 30 min. Whole-cell lysates were prepared and subjected to immunoblot analysis. HepG2 cells (*D*) or primary hepatocytes (*E*) were transfected with or without control siRNA or siRNA targeting hTCPTP for 48 h and then treated with 100 nmol/L GW501516 or DMSO. After incubation for 30 min, the cells were treated with or without 100 nmol/L insulin for a further 30 min. Whole-cell lysates were analyzed by immunoblotting. *F*: HepG2 cells were treated with 100 nmol/L GW501516 or DMSO for 30 min and then exposed to 100 nmol/L insulin for the indicated periods of time. *G*: HepG2 cells transfected with Flag-human PPARδ (Flag-hPPARδ) for 48 h were treated with 100 nmol/L GW501516 or DMSO for 30 min and then exposed to 100 nmol/L insulin for the indicated periods of time. *H*: Immunoblot analyses of *F* and *G* were quantified and represented with DMSO, GW501516, Flag-hPPARδ overexpression + DMSO, and Flag-hPPARδ overexpression + GW501516.

for PPARα and PPARγ, respectively, did not affect insulin-stimulated phosphorylation of IRβ (Supplementary Fig. 4*E* and *F*).

GW501516-Activated PPARδ Regulates IRβ Phosphorylation in a TCPTP45-Dependent Manner

Ectopic expression of TCPTP45 inhibited the effect of GW501516 on IRβ phosphorylation in cells stably expressing PPARδ shRNA but not control shRNA, whereas this effect of GW501516 was rescued by ectopic expression of PPARδ (Fig. 5*A* and Supplementary Fig. 5*A*). Furthermore, the GW501516-stimulated interaction between PPARδ and TCPTP45 demonstrated in PPARδ precipitates was clearly correlated with increased phosphorylation of IRβ (Fig. 5*B*). However, this effect of GW501516 was almost completely abolished in the coimmunoprecipitate of $TCPTP45^{350/378\text{-}A3}$, indicating that the GW501516-stimulated interaction of PPARδ with TCPTP45 prevents the access of TCPTP45 to cytoplasmic tyrosine-phosphorylated IRβ (Fig. 5*C*).

The GW501516-Stimulated Interaction of PPARδ With TCPTP45 Influences Downstream IR Signaling

IR signaling has its biological effects in target organs through phosphorylation of intracellular effector molecules such as IRS-1 and Akt (2). Consistent with the effect of GW501516 on IRβ phosphorylation, GW501516 treatment prolonged the duration of insulin-stimulated IRS-1 and Akt phosphorylation for 6 h in HepG2 cells stably expressing control shRNA (Supplementary Fig. 5*B*), whereas these effects of GW501516 were dramatically inhibited in the presence of PPARδ shRNA (Fig. 5*D*). In addition, the GW501516-stimulated interaction of PPARδ with TCPTP45 observed in PPARδ precipitates was correlated with the increased phosphorylation of IRS-1 and Akt; however, these effects of GW501516 were almost completely abolished when $TCPTP45^{350/378\text{-}A3}$ was coimmunoprecipitated, indicating that the interaction between PPARδ and TCPTP45 directly correlates with IRS-1 and Akt phosphorylation (Fig. 5*E*).

We next assessed glucose levels in the HepG2 cells to evaluate whether GW501516-mediated activation of PPARδ is directly coupled to the biological effects of insulin. Upon exposure to insulin for 30 min, glucose levels in the glucose production medium dramatically decreased, and this reduction in glucose output was further enhanced by treatment with GW501516 in HepG2 cells stably expressing control shRNA. However, this effect of GW501516 on glucose levels in the glucose production medium was significantly inhibited in cells stably expressing PPARδ shRNA (Fig. 5*F*).

GW501516-Activated PPARδ Regulates Insulin Signaling in Myotubes and Adipocytes

Because skeletal muscle and adipocytes are also major target organs of insulin action (1), we investigated the effect of GW501516 on insulin signaling in differentiated mouse C2C12 myotubes and 3T3-L1 adipocytes. Consistent with the results observed in HepG2 cells, GW501516 also increased the duration of IRβ and Akt phosphorylation by promoting interaction between PPARδ and TCPTP45 (Fig. 6*A* and *B* and Supplementary Fig. 6*A* and *B*). Similar results were also observed in C2C12 myotubes transfected with epitope-tagged PPARδ and TCPTP45, whereas the effects of GW501516 on the interaction of PPARδ with TCPTP45 and insulin signaling were almost completely abolished in C2C12 myotubes transfected with epitope-tagged PPARδ and $TCPTP45^{350/378\text{-}A3}$ (Supplementary Fig. 6*C*). Furthermore, insulin-induced translocation of Glut4 to the plasma membrane was sustained for 6 h in cells treated with both insulin and GW501516, whereas the Glut4 signal was predominantly cytoplasmic in cells treated with insulin alone at this time point (Fig. 6*C* and *D*).

The GW501516-Stimulated Interaction Between PPARδ and TCPTP45 Mitigates IL-6–Induced Insulin Resistance

Because obesity-associated chronic inflammation of adipose tissue leads to insulin resistance in peripheral tissues, including the liver, and TCPTP45 is implicated in glucose homeostasis through STAT3 signaling in the liver (10,19), we examined the effects of GW501516 on IL-6–induced insulin resistance. Insulin enhanced the phosphorylation of IRS-1 and Akt in HepG2 cells, but the insulin-stimulated phosphorylation of IRS-1 and Akt was markedly attenuated in the presence of IL-6. However, this IL-6–mediated suppression of IRS-1 and Akt phosphorylation was reversed by GW501516, implying a possible role for PPARδ in the antagonism of inflammation-induced insulin resistance (Fig. 6*E*).

Because STAT3 and SOCS3 are implicated in IL-6–induced insulin resistance (12,20), we examined the effects of GW501516 on the activation and expression of STAT3 and SOCS3. Insulin-stimulated phosphorylation of STAT3 and expression of SOCS3 were inhibited in HepG2 cells stably expressing control shRNA in the presence of GW501516, but these effects of GW501516 were substantially prevented by the expression of PPARδ shRNA (Fig. 6*F*). Consistent with these results, siRNA-mediated knockdown of SOCS3 prevented the IL-6–triggered suppression in the phosphorylation of IRS-1 and Akt, indicating that SOCS3

Data are expressed as mean ± SE (n = 3). *$P < 0.01$ vs. DMSO-treated group. #$P < 0.01$ vs. DMSO-treated Flag-hPPARδ group. HepG2 cells stably expressing control shRNA (*I*) or shRNA targeting PPARδ (*J*) were treated with 100 nmol/L GW501516 or DMSO for 30 min and then exposed to 100 nmol/L insulin for the indicated periods of time. *K*: The immunoblots were then quantified and represented with control shRNA + DMSO, control shRNA + GW501516, hPPARδ shRNA + DMSO, and hPPARδ shRNA + GW501516. Results are expressed as mean ± SE (n = 3). *$P <$ 0.01 vs. DMSO-treated control shRNA group. HepG2 cells stably expressing control shRNA (*L*) or shRNA targeting PPARδ (*M*) were transfected with pcDNA-Flag or pcDNA-Flag-hPPARδ for 48 h. The cells were treated with 100 nmol/L GW501516 or DMSO for 30 min and then exposed to 100 nmol/L insulin for a further 30 min. *N*: Immunoblots were then quantified and represented with control shRNA or hPPARδ shRNA. Results are expressed as mean ± SE (n = 3). **$P < 0.05$, ##$P < 0.05$.

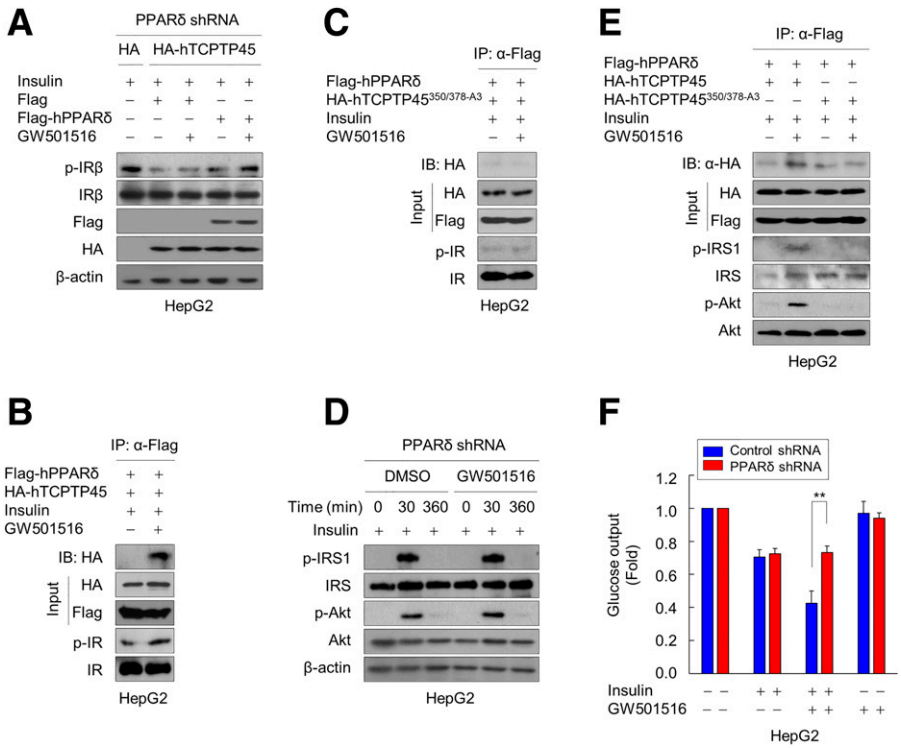

Figure 5—The GW501516-stimulated interaction of PPARδ with TCPTP45 directly affects the insulin receptor. *A*: HepG2 cells stably expressing PPARδ shRNA were cotransfected with pcDNA-HA, pcDNA-human TCPTP45 (HA-hTCPTP45), pcDNA-Flag, and/or pcDNA-Flag-human PPARδ (Flag-hPPARδ) for 48 h. The cells were treated with 100 nmol/L GW501516 or DMSO for 30 min and then exposed to 100 nmol/L insulin for a further 30 min. Whole-cell lysates were analyzed by immunoblotting (IB). IP, immunoprecipitation; p-, phosphorylated. HepG2 cells cotransfected with pcDNA-Flag-hPPARδ and pcDNA-HA-hTCPTP45 (*B*) or pcDNA-HA-hTCPTP45$^{350/378\text{-}A3}$ (*C*) for 48 h were treated with 100 nmol/L GW501516 or DMSO for 30 min and then exposed to 100 nmol/L insulin for a further 30 min. Cell lysates were then immunoprecipitated with anti-Flag antibody and analyzed by immunoblotting. *D*: HepG2 cells stably expressing PPARδ shRNA were treated with 100 nmol/L GW501516 or DMSO for 30 min and then exposed to 100 nmol/L insulin for the indicated periods of time. Whole-cell lysates were analyzed by immunoblotting. *E*: HepG2 cells cotransfected with pcDNA-Flag-hPPARδ and pcDNA-HA-hTCPTP45 or pcDNA-HA-hTCPTP45$^{350/378\text{-}A3}$ for 48 h were treated with 100 nmol/L GW501516 or DMSO for 30 min and then exposed to 100 nmol/L insulin for a further 6 h. Whole-cell lysates were immunoprecipitated and analyzed by immunoblotting. *F*: HepG2 cells stably expressing shRNA against control or PPARδ were treated with 100 nmol/L GW501516 or DMSO for 30 min. After exposure to 100 nmol/L insulin for 8 h, the quantity of glucose present in the glucose production medium was determined and represented with control shRNA or hPPARδ shRNA. Results are expressed as mean ± SE (n = 3). $^{**}P < 0.05$.

plays a role in the GW501516-dependent modulation of insulin resistance induced by IL-6 (Supplementary Fig. 6*D*). In addition, GW501516-stimulated interaction between PPARδ and TCPTP45 observed in PPARδ precipitates was directly correlated with the increased phosphorylation of Akt, with concomitant reductions in the levels of STAT3 phosphorylation and SOCS3 expression. However, these effects of GW501516 were significantly blunted in cells transfected with TCPTP45$^{350/378\text{-}A3}$ instead of TCPTP45, indicating that the GW501516-stimulated interaction of PPARδ with TCPTP45 improves IL-6–induced insulin resistance by targeting STAT3 and SOCS3 (Fig. 6*G*). Similar results were also observed in primary hepatocytes (Fig. 6*H*).

Administration of GW501516 Enhances Insulin Signaling in Animal Models

We next wished to evaluate whether GW501516-activated PPARδ can affect glucose metabolism in ND- or HFD-fed mice. In follow-up experiments, we fed mice an ND or HFD for 10 weeks and checked their body masses weekly to confirm the expected effect of HFD feeding (Supplementary Fig. 7*A*). When mice were administered with GW501516 or DMSO and challenged 30 min later with a bolus of glucose by intraperitoneal injection, blood glucose levels of ND- or HFD-fed mice rapidly increased to peak 30 min later. However, blood glucose subsequently decreased more rapidly in HFD-fed mice that had been administered with GW501516 than in those that had not (Fig. 7*A*). Analogous results were obtained in HFD-fed mice subjected to IPITT, in which the insulin-stimulated decrease in blood glucose was greater after GW501516 administration (Fig. 7*B*).

To determine whether the administration of GW501516 directly affected the interaction between PPARδ and TCPTP45, leading to an improvement of insulin signaling in vivo, we analyzed the interaction by coimmunoprecipitation in lysates prepared from liver, skeletal muscle, and adipose

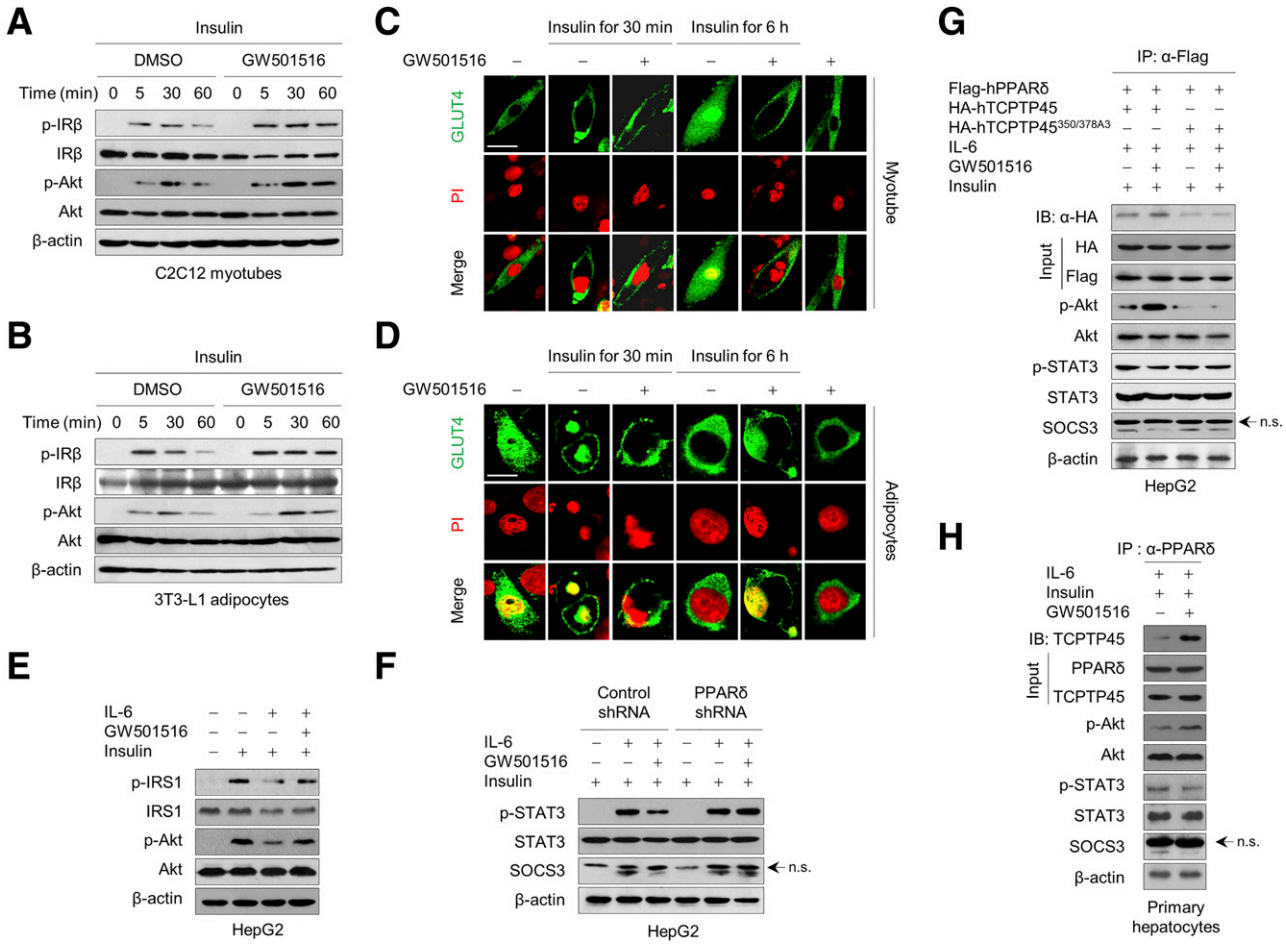

Figure 6—GW501516-activated PPARδ modulates downstream insulin sensitivity and resistance through its interaction with TCPTP45. Differentiated C2C12 myotubes (*A* and *C*) or 3T3-L1 adipocytes (*B* and *D*) were treated with 100 nmol/L GW501516 or DMSO for 30 min and then exposed to 100 nmol/L insulin for the indicated periods of time. The cells were subjected to immunoblot (IB) (*A* and *B*) or fluorescence image analysis (*B* and *D*). For Glut4 translocation assay, the fixed cells were sequentially reacted with primary anti-Glut4 antibody and Alexa Fluor 488–conjugated secondary antibody, and the fluorescent signals were visualized. Nuclei were stained with propidium iodide (PI). p-, phosphorylated. Scale bars = 20 μm. *E*: HepG2 cells treated with or without 20 ng/mL IL-6 for 90 min were incubated with 100 nmol/L GW501516 or DMSO for 30 min and then exposed to 100 nmol/L insulin for a further 30 min. The cells were lysed and analyzed by immunoblotting. *F*: HepG2 cells stably expressing control shRNA or shRNA targeting PPARδ were treated with or without 20 ng/mL IL-6 for 90 min. The cells were incubated with 100 nmol/L GW501516 or DMSO for a further 30 min and then exposed to 100 nmol/L insulin for an additional 30 min. Whole-cell lysates were then analyzed by immunoblotting. *G* and *H*: HepG2 cells cotransfected with pcDNA-Flag-human PPARδ (Flag-hPPARδ) and pcDNA-human TCPTP45 (HA-hTCPTP45) or pcDNA-HA-hTCPTP45$^{350/378A3}$ (*G*), or primary hepatocytes (*H*) were treated with or without 20 ng/mL IL-6 for 90 min. n.s., not significant. The cells were then incubated with 100 nmol/L GW501516 or DMSO for a further 30 min and exposed to 100 nmol/L insulin for a final 30 min. Whole-cell lysates were immunoprecipitated (IP) and analyzed by immunoblotting. Two percent of each whole-cell lysate was used as the input.

tissue. The interaction between PPARδ and TCPTP45 was greatest in the tissues of ND-fed mice administered with GW501516, with a lesser effect of GW501516 detected in HFD-fed mouse tissues. This GW501516-mediated enhancement in the PPARδ/TCPTP45 interaction was closely correlated with the phosphorylation levels of IRβ and Akt in these tissues (Fig. 7*C*–*E*). Interestingly, the circulating levels of insulin, glucose, and IL-6 were significantly higher in HFD-fed mice than in ND-fed mice, but the levels of insulin and glucose were significantly lower in mice treated with GW501516 for 30 min (Fig. 7*F* and *G* and Supplementary Fig. 7*B*), implying an important role for PPARδ in insulin action and whole-body glucose homeostasis in vivo.

DISCUSSION

Short-term activation of PPARδ modulates IR signaling by preventing translocation of the IR-specific phosphatase TCPTP45 into the cytoplasm because of their direct protein-protein interaction. Unlike the genomic action of the transcription factor PPARδ, little is known about nongenomic actions of PPARδ, such as its protein-protein interactions. Based on the concept that PPARδ exerts its biological actions by regulating the transcription of target genes (13), recent studies demonstrated that ligand-activated PPARδ improves insulin signaling through transcriptional regulation of target genes such as insulin-induced gene-1, pyruvate dehydrogenase kinase 4, and angiopoietin-like protein 4 in hepatocytes and myotubes (21,22).

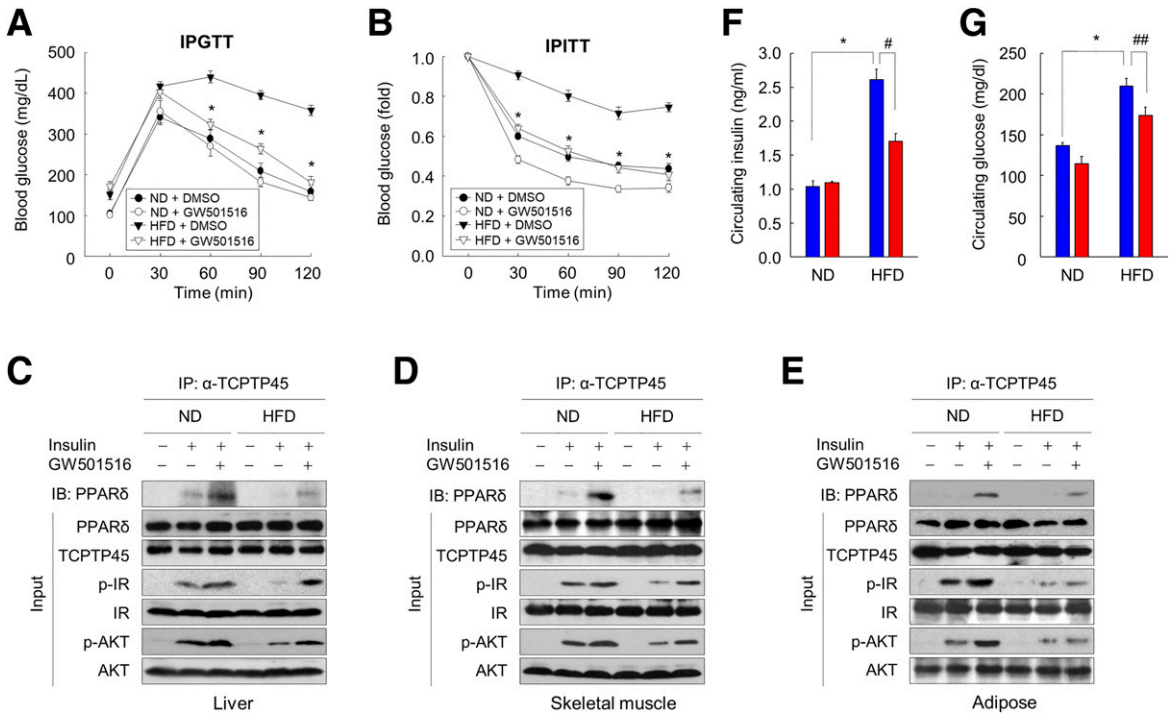

Figure 7—Administration of GW501516 improves in vivo insulin sensitivity and glucose tolerance through its interaction with TCPTP45. Mice fed an ND or HFD for 10 weeks were fasted for 14 h and treated with 10 mg/kg GW501516 or DMSO for 30 min. After an intraperitoneal injection of 2 g/kg glucose or 0.5 units/kg insulin, an intraperitoneal glucose tolerance test (IPGTT) (*A*) or IPITT (*B*) was performed. Blood glucose was measured and represented with ND + DMSO, ND + GW501516, HFD + DMSO, and HFD + GW501516. Data are expressed as mean ± SE (n = 6). *$P < 0.01$ vs. the HFD + DMSO group. Mice fed an ND or HFD for 10 weeks were fasted for 14 h and then treated with 10 mg/kg GW501516 or DMSO for 30 min. After exposure to 0.5 units/kg insulin for 30 min, the mice were sacrificed by inhalation of CO_2 gas, and then liver (*C*), skeletal muscle (*D*), and adipose tissue (*E*) were removed. Tissue homogenates were prepared and immunoprecipitated (IP) with anti-TCPTP45 antibody. The total lysates (input) and immunoprecipitates were analyzed by immunoblotting (IB). Two percent of each tissue lysate was used as the input. p-, phosphorylated. Mice were fed an ND or HFD for 10 weeks and then starved for 14 h. They were then treated with 10 mg/kg GW501516 or DMSO for 30 min and sacrificed. Circulating levels of insulin and glucose were determined by ELISA or spectrometric methods using sera prepared from blood collected from the carotid artery. Data are expressed as mean ± SE (n = 6). *$P < 0.01$, #$P < 0.01$, ##$P < 0.05$.

In the most recent reports, cells were treated with specific PPARδ ligands for as long as 18 to 24 h so that the effect of PPARδ activation on transcriptional programs and downstream biological activities could be investigated (23,24). However, we show here that the activation of PPARδ by GW501516 for only 30 min was sufficient to phosphorylate IRβ and, consequently, IRS-1 and Akt. To achieve this effect, GW501516 promoted the interaction of PPARδ with TCPTP45 but could not affect the transcription of TCPTP45. These findings suggest that nongenomic actions of PPARδ, rather than its genomic actions, are important for the regulation of IR signaling. We thus propose a novel mechanism whereby PPARδ influences insulin signaling by involving the sequestration of PPARδ in the nucleus secondary to a protein-protein interaction with the IRβ-specific phosphatase TCPTP45 and, therefore, prevents binding to its cytoplasmic substrate IRβ.

Although GW501516-activated PPARδ interacted with both TCPTP45 and TCPTP48, it colocalized in the nucleus with TCPTP45 but not TCPTP48. These two alternative splice variants exhibit distinct subcellular localizations because of a difference in the seven amino acid residues at their carboxy-terminals. As a result, TCPTP48 is mainly localized to the ER, whereas TCPTP45 is restricted to the nucleus in resting cells (9). Therefore, TCPTP48 dephosphorylates IRβ after it is endocytosed into the ER in response to insulin, whereas TCPTP45 dephosphorylates IRβ in the cytoplasm and at the plasma membrane after its translocation from the nucleus (6,9). In this context, the PPARδ-mediated prevention of TCPTP45 translocation, but not that of TCPTP48, into the cytoplasm may contribute to the enhancement in insulin signaling. GW501516-activated PPARδ also did not interact with PTP1B, another tyrosine-specific phosphatase that targets IRβ in the ER (4,6). Thus, the subcellular localization, as well as the other biochemical properties of the substrate, when interacting with PPARδ, may be critical determinants of the effects of PPARδ on insulin signaling.

PPARδ, but not PPARα or γ, specifically interacted with TCPTP45 in a ligand-dependent manner to enhance insulin signaling. Previous studies demonstrated that specific ligands for PPARγ enhance insulin signaling through genomic actions regulating gene transcription, including that of adipocyte P2 (aP2), lipoprotein lipase (LPL), fatty

acid-transport protein (FATP), Glut4, glucokinase, uncoupling protein (UCP)-2 and UCP-3, to regulate glucose homeostasis, adipocyte differentiation, and lipid storage in cell or animal models (25,26). Ligand-activated PPARα also ameliorated insulin resistance by upregulating genes encoding FATP, acyl-CoA oxidase, and LPL, leading to increased hepatic fatty acid uptake and lipid metabolism (27,28). These findings are consistent with the data reported here because both enhance insulin signaling, but the underlying mechanisms mediating this effect are specific to the PPAR isoform. Indeed, only a 30-min treatment with GW501516 was sufficient to activate PPARδ and enhance insulin signaling by inhibiting translocation of the IRβ-specific phosphatase TCPTP45 into the cytoplasm. This was the result of a direct interaction with TCPTP45, which we term a nongenomic action here. Consequently, the effect of each PPAR nuclear receptor on insulin signaling can be characterized according to its genomic and/or nongenomic actions.

Although the present findings are consistent with previous reports that GW501516-activated PPARδ ameliorates IL-6–induced insulin resistance in hepatocytes by inhibiting the STAT3-SOCS3 pathway (29), the molecular mechanisms may differ between studies because the 30-min treatment with GW501516 was sufficient to inactivate the STAT3-SOCS3 pathway in this study. Several recent studies demonstrated that activation of PPARδ by specific ligands alleviated IL-6–induced insulin resistance by suppressing SOCS3 expression, secondary to inhibition of STAT3 activation. These effects of GW501516 were observed in hepatocytes and adipocytes treated for 24 h, suggesting that the effects of PPARδ in this context may be principally dependent on its genomic activity (30,31). Indeed, TCPTP45 was reported to inhibit IL-6–induced STAT3 phosphorylation, leading to the attenuation of insulin signaling in the liver (10,11). Consistent with these reports, PPARδ-mediated retention of TCPTP45 in the nucleus facilitated the access of TCPTP45 to its substrate STAT3, resulting in reduced IL-6–mediated phosphorylation and suppression of STAT3-mediated SOCS3 expression, which is linked to insulin resistance (19,29). Thus, the insulin-sensitizing effects of GW501516 may be collectively mediated by the interaction between PPARδ and TCPTP45.

Contrary to our present findings showing the TCPTP45-dependent effect of PPARδ in insulin signaling, a previous study demonstrated that TCPTP deficiency in muscle has no effect on insulin signaling and glucose homeostasis (32). Although this discrepancy for TCPTP action in muscle insulin signaling is not fully elucidated at present, our present data evenly showed that the GW501516-dependent interaction of PPARδ and TCPTP45 potentiated the insulin-triggered phosphorylation of IRβ and Akt and translocation of Glut4 in C2C12 myotubes. In fact, previous studies reported that ligand-activated PPARδ ameliorates cellular energy homeostasis through its genomic action regulating transcription of genes, including UCP-2, UCP-3, pyruvate dehydrogenase kinase 4, carnitine palmitoyltransferase 1, and malonyl-CoA decarboxylase in skeletal muscle (13,22–25). Thus, the possibility remains that the effects of PPARδ activation on the insulin signaling may be attributed to their transcriptional regulation of multiple genes rather than to direct interaction of PPARδ and TCPTP45 in C2C12 myotubes. Further studies are necessary to clarify the exact molecule(s) associated with PPARδ-mediated insulin signaling in muscle.

Consistent with the in vitro data, mice exposed to GW501516 for as little as 30 min showed enhanced insulin-stimulated phosphorylation of IRβ and Akt in the liver, skeletal muscle, and adipose tissue. This GW501516-mediated enhancement in insulin signaling and glucose homeostasis, which occurred even in HFD-fed obese mice, was accompanied by greater interaction between PPARδ and TCPTP45, indicating that these in vivo effects of GW501516 are dependent on the association between PPARδ with TCPTP45, as in the cell models. A number of studies to date have shown that activation of PPARδ regulates insulin signaling by regulating the expression of genes involved in lipid and glucose homeostasis. However, the current study implies that PPARδ has multiple modes of action and can enhance insulin signaling through an interaction with TCPTP45, which we characterized as a nongenomic action. These findings may suggest novel alternative future therapeutic strategies for disorders related to defective insulin signaling.

Funding. This work was supported in part by the Basic Science Research Program through the National Research Foundation of Korea (NRF), funded by the Ministry of Science, ICT and Future Planning (NRF-2017R1A2A2A05001249 and NRF-2015R1A5A1009701), and by the Next-Generation BioGreen 21 Program (no. PJ01122201), Rural Development Administration, Republic of Korea.

Duality of Interest. No potential conflicts of interest relevant to this article were reported.

Author Contributions. T.Y., S.A.H., W.J.L., S.I.H., J.-A.P., J.S.H., J.H., H.-C.S., S.G.H., C.-H.L., and D.W.H. performed the experiments. T.Y., K.S.P., and H.G.S. analyzed the results and wrote the manuscript. T.Y. and H.G.S. conceived and designed the experiments. T.Y. and H.G.S. are the guarantors of this work and, as such, had full access to all the data in the study and take responsibility for the integrity of the data and the accuracy of the data analysis.

References

1. Saltiel AR, Kahn CR. Insulin signalling and the regulation of glucose and lipid metabolism. Nature 2001;414:799–806

2. White MF. The IRS-signalling system: a network of docking proteins that mediate insulin action. Mol Cell Biochem 1998;182:3–11

3. Kahn SE, Hull RL, Utzschneider KM. Mechanisms linking obesity to insulin resistance and type 2 diabetes. Nature 2006;444:840–846

4. Bourdeau A, Dubé N, Tremblay ML. Cytoplasmic protein tyrosine phosphatases, regulation and function: the roles of PTP1B and TC-PTP. Curr Opin Cell Biol 2005;17:203–209

5. Tiganis T. PTP1B and TCPTP–nonredundant phosphatases in insulin signaling and glucose homeostasis. FEBS J 2013;280:445–458

6. Galic S, Hauser C, Kahn BB, et al. Coordinated regulation of insulin signaling by the protein tyrosine phosphatases PTP1B and TCPTP. Mol Cell Biol 2005;25:819–829

7. Cool DE, Tonks NK, Charbonneau H, Walsh KA, Fischer EH, Krebs EG. cDNA isolated from a human T-cell library encodes a member of the protein-tyrosine-phosphatase family. Proc Natl Acad Sci U S A 1989;86:5257–5261

8. Lorenzen JA, Dadabay CY, Fischer EH. COOH-terminal sequence motifs target the T cell protein tyrosine phosphatase to the ER and nucleus. J Cell Biol 1995;131: 631–643
9. Lam MH, Michell BJ, Fodero-Tavoletti MT, Kemp BE, Tonks NK, Tiganis T. Cellular stress regulates the nucleocytoplasmic distribution of the protein-tyrosine phosphatase TCPTP. J Biol Chem 2001;276:37700–37707
10. Fukushima A, Loh K, Galic S, et al. T-cell protein tyrosine phosphatase attenuates STAT3 and insulin signaling in the liver to regulate gluconeogenesis. Diabetes 2010;59:1906–1914
11. Yamamoto T, Sekine Y, Kashima K, et al. The nuclear isoform of protein-tyrosine phosphatase TC-PTP regulates interleukin-6-mediated signaling pathway through STAT3 dephosphorylation. Biochem Biophys Res Commun 2002;297:811–817
12. White AT, LaBarge SA, McCurdy CE, Schenk S. Knockout of STAT3 in skeletal muscle does not prevent high-fat diet-induced insulin resistance. Mol Metab 2015;4: 569–575
13. Neels JG, Grimaldi PA. Physiological functions of peroxisome proliferator-activated receptor β. Physiol Rev 2014;94:795–858
14. Mansour M. The roles of peroxisome proliferator-activated receptors in the metabolic syndrome. Prog Mol Biol Transl Sci 2014;121:217–266
15. Krogsdam AM, Nielsen CA, Neve S, et al. Nuclear receptor corepressor-dependent repression of peroxisome-proliferator-activated receptor delta-mediated transactivation. Biochem J 2002;363:157–165
16. Ham SA, Kang ES, Lee H, et al. PPARδ inhibits UVB-induced secretion of MMP-1 through MKP-7-mediated suppression of JNK signaling. J Invest Dermatol 2013; 133:2593–2600
17. Eguchi A, Furusawa H, Yamamoto A, et al. Optimization of nuclear localization signal for nuclear transport of DNA-encapsulating particles. J Control Release 2005; 104:507–519
18. Tiganis T, Bennett AM, Ravichandran KS, Tonks NK. Epidermal growth factor receptor and the adaptor protein p52Shc are specific substrates of T-cell protein tyrosine phosphatase. Mol Cell Biol 1998;18:1622–1634
19. Senn JJ, Klover PJ, Nowak IA, et al. Suppressor of cytokine signaling-3 (SOCS-3), a potential mediator of interleukin-6-dependent insulin resistance in hepatocytes. J Biol Chem 2003;278:13740–13746
20. Galic S, Sachithanandan N, Kay TW, Steinberg GR. Suppressor of cytokine signalling (SOCS) proteins as guardians of inflammatory responses critical for regulating insulin sensitivity. Biochem J 2014;461:177–188
21. Qin X, Xie X, Fan Y, et al. Peroxisome proliferator-activated receptor-delta induces insulin-induced gene-1 and suppresses hepatic lipogenesis in obese diabetic mice. Hepatology 2008;48:432–441
22. Ordelheide AM, Heni M, Thamer C, et al. In vitro responsiveness of human muscle cell peroxisome proliferator-activated receptor δ reflects donors' insulin sensitivity in vivo. Eur J Clin Invest 2011;41:1323–1329
23. Lee CH, Olson P, Hevener A, et al. PPARdelta regulates glucose metabolism and insulin sensitivity. Proc Natl Acad Sci U S A 2006;103:3444–3449
24. Chen W, Wang LL, Liu HY, Long L, Li S. Peroxisome proliferator-activated receptor delta-agonist, GW501516, ameliorates insulin resistance, improves dyslipidaemia in monosodium L-glutamate metabolic syndrome mice. Basic Clin Pharmacol Toxicol 2008;103:240–246
25. Spiegelman BM, Flier JS. Obesity and the regulation of energy balance. Cell 2001;104:531–543
26. Evans RM, Barish GD, Wang YX. PPARs and the complex journey to obesity. Nat Med 2004;10:355–361
27. Aoyama T, Peters JM, Iritani N, et al. Altered constitutive expression of fatty acid-metabolizing enzymes in mice lacking the peroxisome proliferator-activated receptor alpha (PPARalpha). J Biol Chem 1998;273:5678–5684
28. Kersten S, Seydoux J, Peters JM, Gonzalez FJ, Desvergne B, Wahli W. Peroxisome proliferator-activated receptor alpha mediates the adaptive response to fasting. J Clin Invest 1999;103:1489–1498
29. Kim JH, Kim JE, Liu HY, Cao W, Chen J. Regulation of interleukin-6-induced hepatic insulin resistance by mammalian target of rapamycin through the STAT3-SOCS3 pathway. J Biol Chem 2008;283:708–715
30. Serrano-Marco L, Rodríguez-Calvo R, El Kochairi I, et al. Activation of peroxisome proliferator-activated receptor-β/-δ (PPAR-β/-δ) ameliorates insulin signaling and reduces SOCS3 levels by inhibiting STAT3 in interleukin-6-stimulated adipocytes. Diabetes 2011;60:1990–1999
31. Serrano-Marco L, Barroso E, El Kochairi I, et al. The peroxisome proliferator-activated receptor (PPAR) β/δ agonist GW501516 inhibits IL-6-induced signal transducer and activator of transcription 3 (STAT3) activation and insulin resistance in human liver cells. Diabetologia 2012;55:743–751
32. Loh K, Merry TL, Galic S, et al. T cell protein tyrosine phosphatase (TCPTP) deficiency in muscle does not alter insulin signalling and glucose homeostasis in mice. Diabetologia 2012;55:468–478